International Journal of Engineering, Construction and Computing
Volume 1 Issue 1, 2019
ISSN: 2209-332X(Print)

Experimental study of bending stiffness variation during a full rotation of cracked shafts

Erfan Taheri, Helen Wu and Ming Zhao
School of Computing, Engineering and Mathematics, Western Sydney University, Australia.
*Corresponding author's email: 17783747@student.westernsydney.edu.au

Peer review history

Manuscript submitted: 7 June 2019
Review process completed: 18 July 2019
Manuscript finally accepted: 25 July 2019
Handling Editor: Professor Ataur Rahman

Abstract: *The mechanical shaft is a key element in the majority of mechanical systems. It is responsible for delivering power from one end of the drive train to another. The rotating shaft undergoes rapid fluctuations of bending moment stresses and when combined with their long operational hours, it can eventually form a crack and thus lead to shaft failure. Therefore, it is imperative that a method is developed in order to detect cracks whilst the shaft is in motion. In this paper, an experimental analysis is conducted to obtain the bending stiffness values, and to contribute to the literature of rotor-dynamics so that eventually a method for early crack detection during dynamic operation can be developed. The experimental research involves the creation of cracked shaft models (0.1 mm wire cutting into the shaft, 0.3 mm wire cutting into the shaft, having two 0.3 mm wire cutting into the shaft and developing a 0.3 mm crack by welding joinery). This method of creating the cracked shaft models is relatively quick, easy and cost effective. A three-point-bending test is then conducted on the cracked shaft models to evaluate the shaft's stiffness variation through varying angular positions. The results show that all the cracked shaft models exhibit the breathing mechanism corresponding to the cracks location during rotation.*

Keywords: *Cracked; Shaft; Rotor; Dynamics; Breathing.*

1. Introduction

Mechanical shafts are present in almost every mechanical system, including motor vehicles, aircrafts, boats, mining equipment etc. Due to the shaft's dynamic nature, it is prone to experiencing internal forces, rapid changes in bending moments, stresses and tension forces. These constant forces acting on the shaft may contribute to the formation of cracks. When a shaft develops a crack, it may go unnoticed and eventually lead to shaft failure. Shaft failure occurs when the shaft breaks into two or more pieces. As most industrial processes rely upon a form of mechanical machinery, it is important to be able to detect a crack in a shaft, prior to the onset of failure. Shaft failure could lead to injuries and potential fatalities, i.e. failure occurring in an aircraft engine.

Many large-scale industries such as mining, agriculture and manufacturing factories heavily rely on their machinery for business operation and generating revenue. If shaft failure occurs, then the outcome would be costly causing delays and loss of revenue. There are no current methods for detecting a crack in a shaft whilst the shaft is in operation. Therefore, this topic serves as one of the most important issues in rotor dynamics and a solution will inevitably save on costs, reduce fatal accidents and avoid injuries.

An interesting phenomenon, known as crack breathing, occurs when analysing the dynamic motion of a cracked shaft. The moving rotation of a shaft also means that the respective location of the crack is also moving. The cracked portion rotates through two distinct regions, a region of compression and a region of tension. When the crack is in a compression zone, then the crack is closed and conversely, when the crack is in a tension zone, it is considered fully open. As the crack goes from being in a compressive zone (closed) to a tension zone (fully open), the gap (of the crack) gradually starts closing until it is in a full compressed zone. Subsequently, when the crack goes from the compression zone to the tension zone, it starts to gradually open until it is completely open. This process keeps repeating for every 360-degree rotation. Thus as the shaft is rotating, the crack is constantly changing how much it is open and closed, and this phenomenon is referred to as the "crack breathing" mechanism (Georgantzinos et al., 2008). This constant changing phenomenon adds a layer of difficulty to being able to predict a crack prior to it reaching failure.

Al-Shufeifat and Butcher (2011) researched the effects of cracked shafts using analytical, experimental and mathematical methods. They also discuss a mechanical system that can be modelled by three components, i.e. mass, stiffness value and damping factor. It was noted that when a crack is formed in a shaft, the actual mass of the shaft is not affected (negligible) and the damping factor is not affected either. The primary variable which changes is the stiffness value and thus when physically experimenting on shaft models, then the factor of interest would be its stiffness value (Jun, et al., 2008). As the shafts gap is constantly changing during a full revolution (crack breathing phenomenon), then testing the stiffness value at different angles, relative to the crack's starting position, will provide data on the crack breathing phenomenon and the effect on a cracked shaft's stiffness.

It will be possible to test the breathing phenomenon for certain models and to derive new data by experimentally testing for the fluctuating levels of stiffness as the shaft undergoes rotations. The testing would involve creating several models of cracked shafts through methods of wire cutting and welding. Once the cracked shaft models have been formed, then a three-point bending stress machine is used to calculate the deflection of the crack under a certain load. The shaft would have the load applied to it every 30 degrees for a full 360-degree revolution.

2. Methodology

2.1 Creating cracked shaft models

There had to be various models of cracked shafts made in order to conduct a stiffness study. The shaft models experimented on are 85 cm long circular shafts made of AISI 1040 Steel. The shafts have a 19 mm diameter. A wire-cut was performed to make the first model; this was done by using a very thin wire (0.3 mm wide). Figure 1 below shows the Funac wire-cutting apparatus A single strand of wire (composed of 65% copper and 35% zinc) is used to cut the shaft in the centre of it (42.5 cm from either edge inwards). The cut was performed at 40% of the shaft's diameter (cutting 7.6 mm into the shaft). The next shaft was prepared exactly the same way as the previous shaft but with an additional cut, as seen in Figure 2 below. An additional shaft was used for a 0.1 mm wide wire-cut (also cut once in the centre of the shaft and the cut being 40% of the shafts diameter). Figure 3 below shows an enlarged image of the wire-cutting process, there is deionized water being poured on the cut area whilst the single strand is making the cut to ensure there is no overheating.

Figure 1. Fanuc wire-cutting Machine

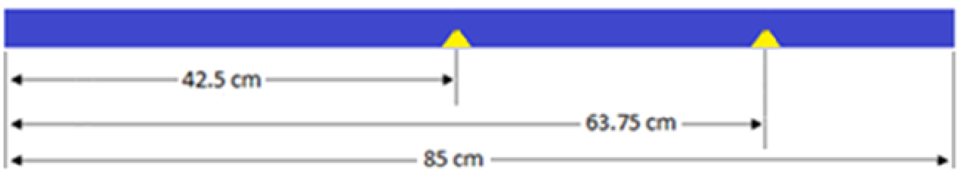

Figure 2. Diagram of shaft with cutting dimensions

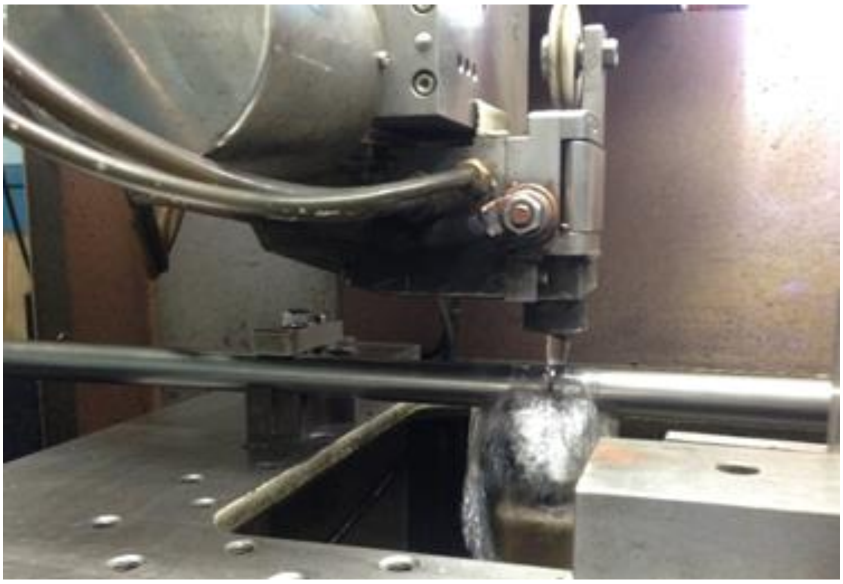

Figure 3. Enlarged view of 0.1 mm wire-cutting process

A fifth shaft was used to make the last cracked model. This method aimed to make the smallest gap possible and it was acquired by using a welding technique. Figure 4 below, shows the main stages in developing the welding crack. The steps in creating a welding crack were firstly, the shaft was cut in half. The amount of crack wanted was 40% of the shafts diameter (19 mm) which equates to 7.6 mm. Therefore, a milling process was used to cut out 11.4 mm from both ends of the shaft. Use a donor shaft to cut out the material to the shape that was cut out of both halves of the shaft but this time having it as one piece. Place the two halves together and weld around the donor piece and the two halves to join them together. The two halves will be pushed together and then a very minute crack is formed. The development of the welding crack is shown in Figure 4 below with (a) showing the shaft halved and milled, (b) showing the donor piece and (c) representing the area that is being welded in red and the yellow line showing the minute welding crack. The welding crack represents the smallest crack model (measured at around 0.03 mm). All the cracked shaft models are shown in Figure 5 below.

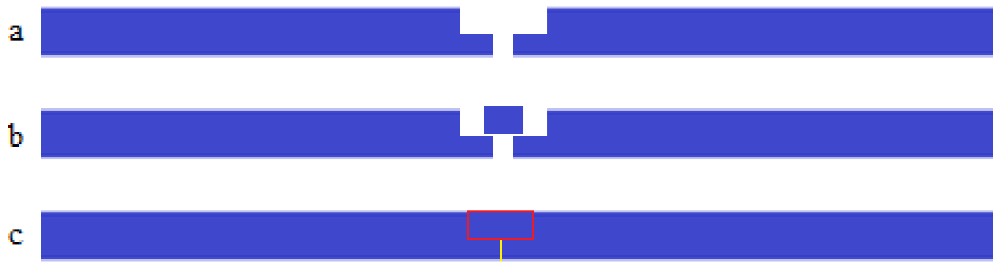

Figure 4. Procedure of welding crack (a) two halves milled (b) donor piece (c) welded together (red lines) and yellow representing 0.03 mm welding crack

Figure 5. (a) 0.3 mm wire-cut crack (b) 0.1 mm wire-cut crack (c) 0.03 mm welding crack (d) two 0.3 mm wire-cut cracks

2.2 Experimental set up and testing

To experiment on the shafts, it was necessary to use a machine that is capable of producing a force and then measuring the deflection caused by the force. The Instron 3365 machine was selected to perform this task. The type of test needed was a three-point bending test, where the shaft sits on two points and a force point is applied in-between the two points the shaft is held in. Figure 6 shows the shaft in the three-point-bending apparatus, with the force being applied to the centre of the shaft (crack location). The supports are located 5 cm on either side of the centre of the shaft. Each shaft, including an intact one as the control, was placed on the machine. The goal of the experiment is to observe the changes in stiffness as the shaft undergoes rotation. When the shaft was placed into the machine, the orientation of the shaft relative to the crack was important, and the initial position was the crack facing upwards. The crack facing upwards was selected as 0 degrees, and every 30 degree was marked on the shaft from the starting 0-degree position. A force of 3000 Newton was then applied, and the deflection was measured. This was done from 0 to 330 degrees at 30-degree intervals. Once the deflection is measured for each shaft (Intact, 0.1 mm wire cut, 0.3 mm wire cut, 2x 0.3 mm wire-cuts and welding crack) at twelve different angles for each one, then it would be possible to graph the stiffness effects, due to the different angles in the various cracked shaft models.

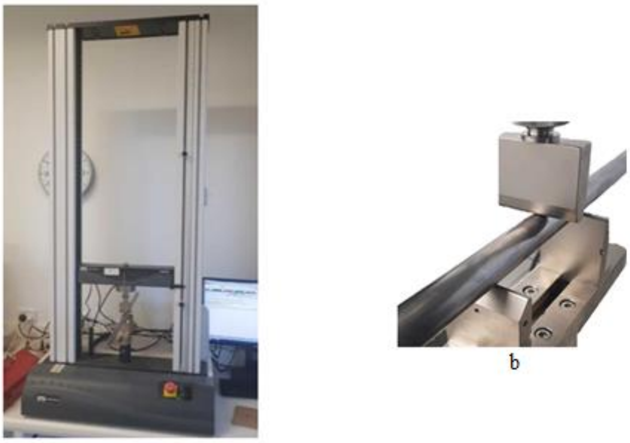

a

b

Figure 6. (a) Three-point bending test using Instron 3365 (b) Enlargement of testing section

Table 1. Stiffness values (0.1 mm wire-cut crack)

Rotation angle θ (Degree)	Force (N)	Deflection $\times 10^3$ (m)	Stiffness (N/m)
0	3000	0.279	12.940
30	3000	0.274	13.047
60	3000	0.264	13.090
90	3000	0.240	13.056
120	3000	0.236	13.143
150	3000	0.257	13.038
180	3000	0.262	13.116
210	3000	0.254	13.266
240	3000	0.236	13.372
270	3000	0.241	13.209
300	3000	0.262	13.182
330	3000	0.274	12.956
360	3000	0.279	12.940

3. Results and discussion

The three-point bending stress was performed on every shaft. At every 30-degree interval there was a force applied in the middle of the shaft, until it reached a maximum load of 3000 Newtons, and at that point, the deflection of the shaft was measured. Table 1 shows the deflection which occurred due to the 3000 Newton force at every angle interval for the 0.1 mm wire-cut crack. The stiffness was then calculated by dividing the maximum force of 3000 newtons by the deflection in metres. Table 2 shows the stiffness for the rest of the shafts that were experimented on.

The stiffness values at varying angular positions were graphed for each shaft, as depicted in Figure 7. For the Intact shaft, as there is no crack, it is expected that the stiffness should not change no matter which angle it is placed at. The stiffness differs with a standard deviation of 0.130 (N/m) from the minimum stiffness being 12.940 (N/m) and the maximum being

13.372 (N/mm). The experimental result gathered is considered accurate and only in theoretical testing could a straight line be achieved.

It is known that the breathing mechanism takes place as the cracked portion of the shaft rotates throughout zones of compression and tension. For the 0.1 mm wire-cut crack, Figure 7 shows a pattern that is symmetrical at nearly 180 degrees which validates that the experimental data obtained is correct and a breathing effect is seen. As the rotation angle continues, the stiffness is seen increasing (peaking at 120 degrees) and then decreasing until it reaches halfway (180 degrees) and the pattern is repeated from 180 degrees to 360 degrees.

Table 2. Stiffness values for shafts

Rotation angle θ (Degree)	Intact shaft (N/m)	Stiffness (N/m) 0.1 mm wire-cut crack	Stiffness (N/m) 0.3 mm wire-cut crack	Stiffness (N/m) Welding crack	Stiffness (N/m) two 0.3 mm wire-cut cracks
0	12.940	10.753	10.909	11.499	10.969
30	13.047	10.949	10.791	11.714	10.897
60	13.090	11.385	10.753	12.000	11.853
90	13.056	12.495	12.898	12.448	12.937
120	13.143	12.701	12.320	12.151	12.341
150	13.038	11.664	11.802	10.870	11.763
180	13.116	11.450	11.173	10.156	11.364
210	13.266	11.830	11.806	10.642	11.990
240	13.372	12.706	12.146	11.806	12.886
270	13.209	12.428	12.842	12.443	13.106
300	13.182	11.450	10.616	12.157	11.025
330	12.956	10.949	10.826	12.082	10.625
360	12.940	10.753	10.909	11.499	10.969

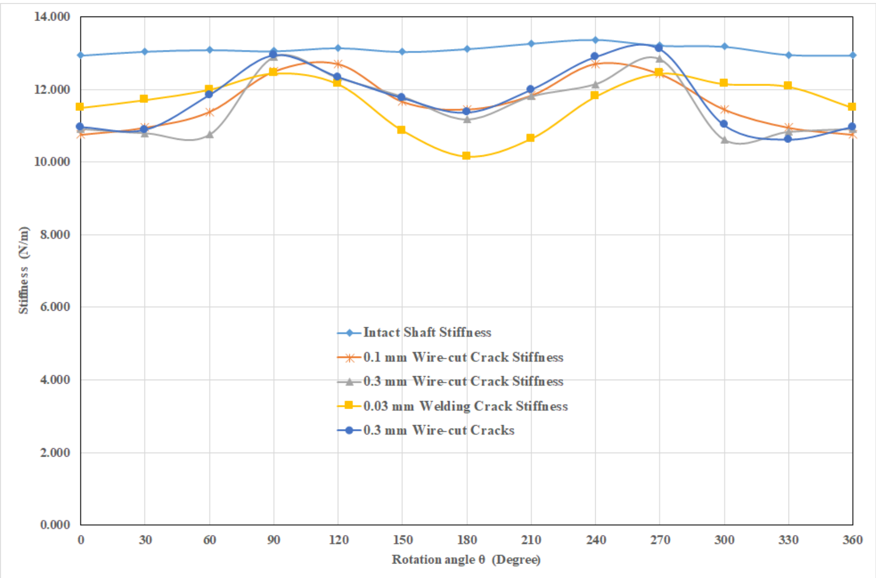

Figure 7. Shaft stiffness values at varying angular positions

For the 0.3 mm wire-cut crack, the graph in Figure 7 shows a pattern that is symmetrical at nearly 180 degrees which validates that the experimental data obtained is correct and a breathing effect was seen. As the rotation angle continues, the stiffness slightly dips and is then seen increasing until it is peaking at 90 degrees. It then begins decreasing until it reaches halfway (180 degrees) and then peaking again at 270 degrees.

For the welding crack, the graph in Figure 7 shows a pattern that is symmetrical at nearly 180 degrees which suggests that the experimental data obtained is correct as a breathing effect is seen. As the rotation angle starts, the stiffness is seen to slightly increase until a peak is reached at 120 degrees. It slowly dips until the minimum stiffness at 180 degrees and then the pattern is mirrored with it rising again and peaking at 270 degrees.

For the two 0.3 mm wire-cut cracks, the graph in Figure 7 shows a pattern that is symmetrical at nearly 90 degrees which suggests that the experimental data obtained is correct as a breathing effect is seen. As the rotation angle starts the stiffness is seen to slightly increase until a peak is reached at 90 degrees. It slowly dips until the minimum stiffness reaches 180 degrees and then the pattern is mirrored with it rising again and peaking at 270 degrees.

The intact shaft behaved as expected within experimental testing and showed minimum stiffness changes despite its angular position. The cracked shaft models all depicted the trend of the stiffness increasing and decreasing until 180 degrees, where the pattern is then repeated in a mirror image. All the shafts displayed symmetrical curvature, confirming the ‘crack breathing’ phenomenon. As the shafts with a crack rotate through a tension zone, it is expected that the stiffness at that point should match closely to the stiffness of the intact shaft (the crack is considered closed, and thus the stiffness should be similar to the intact shaft which has no crack).

4. Conclusion

The research objectives were to find out the correlation a cracked shaft has on stiffness study with varying crack parameters. Firstly, models of cracked shafts had to be developed and they were done so from wire cutting (0.1 mm wire cut, 0.3 mm wire cut and two 0.3 mm wire cuts) and a welding process to form a minute crack (approximately gap of 0.03 mm). Once these models were produced then a force of 3000 newton was applied at the crack location. The shaft was marked at an angle and was rotated every 30 degrees from zero to 360 degrees, thus going through a full revolution. At every 30 degree rotation, the 3000 newton force was applied and the apparatus measured the amount of deflection at that point. The stiffness was then calculated by dividing the force with the deflection and then graphed. The results obtained showed that the graphs where symmetrical at 180 degrees and thus confirming that the experiment was conducted correctly. The physical findings confirmed the theoretical research that a phenomenon known as ‘crack breathing’ occurs when there is a crack present in a shaft. The results obtained are valuable and very important, as the findings are new. The results obtained will lower the research gaps in rotor dynamics and will assist in a method eventually being developed for early crack detection during dynamic shaft operation.

5. Acknowledgements

The authors gratefully acknowledge the financial support from the School of Computing, Engineering, and Mathematics, Western Sydney University, Australia.

6. References

Al-Shudeifat, M. A., & Butcher, E. A. (2011). New breathing functions for the transverse breathing crack of the cracked rotor system: Approach for critical and subcritical harmonic analysis. *Journal of Sound and Vibration*, 330(3), 526-544.

Georgantzinos, S., & Anifantis, N. (2008). An insight into the breathing mechanism of a crack in a rotating shaft. *Journal of Sound and Vibration*, 318(1-2), 279-295.

Jun, O. S., & Gadala, M. S. (2008). Dynamic behavior analysis of cracked rotor. *Journal of Sound and Vibration*, 309(1-2), 210-245.